INDENTED-ANODE DIODE FOR HERMES III*

T. W. L. Sanford, J. W. Poukey, J. A. Halbleib, R. C. Pate,
G. W. Crowder, T. Borkey, F. Current, C. E. Heath, and R. Mock
Sandia National Laboratories, Albuquerque, NM 87185

and

P. W. Spence, V. Bailey, G. A. Proulx, and H. Kishi
Pulse Sciences, Inc., San Leandro, CA 94577

Abstract

Design of three diode configurations that meet the radiation goals of HERMES III and calculation of associated radiation outputs are discussed. These goals are (1) to produce a 20-ns FWHM radiation pulse having a peak dose rate of 5 x 10^{12} rad(Si)/s with a variation of less than a factor of two over a 500 cm^2 irradiation area, (2) to keep the variation less than a factor of four over the irradiation volume defined by extending the area downstream by 15 cm, and (3) to maintain a minimum dose rate over this volume in excess of 2.5 x 10^{12} rad(Si)/s.

Introduction

HERMES III is a 20-MV, 800-kA electron accelerator being constructed at Sandia National Laboratories to produce a large-area, uniform source of pulsed γ-rays [1]. The downstream end of HERMES III will consist of a 30 Ω coaxial MITL [2] (magnetically-insulated transmission line) terminated by a field-emission diode and electron bremsstrahlung radiation target.

In this paper, we discuss the design of coaxial diodes having indented [3] (Fig. 1) and extended planar (Fig. 2) anodes that will be used to efficiently convert the electrical energy of HERMES III into bremsstrahlung radiation to meet the radiation goals of the accelerator [1]. In these diodes, the effective AK (anode-cathode) gap, D1 + R1, controls the diode impedance for a given Rc and Ra for cases where the diode impedance is less than or equal to the self-limited impedance of the MITL [4]; the axial length of the indentation, D2, controls the pinch angle at the target and the subsequent depth uniformity of the downstream radiation pattern; and Rc and R1 control the radial impact position of the beam at the target and

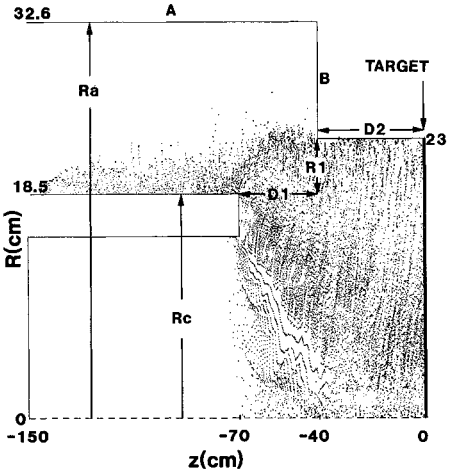

Fig. 1. MAGIC simulation of indented-anode diode corresponding to Configuration 2 of Section III; Ra = 32.6 cm, Rc = 18.5 cm, R1 = 4.5 cm, D1 = 30 cm, D2 = 40 cm; V = 20 MV, I = 710 kA, current loss to side anode wall = 160 kA (23%), $\bar{\theta}$ = 16° ± 4°.

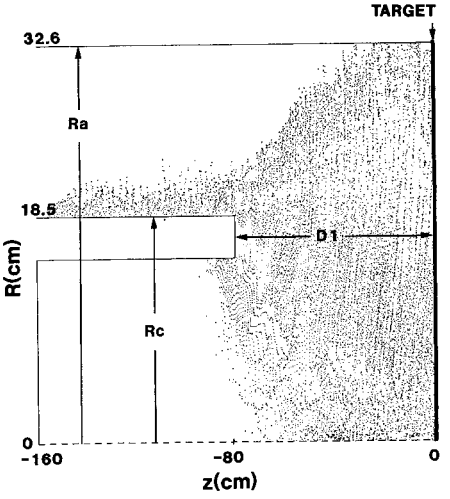

Fig. 2. MAGIC simulation of extended planar-anode diode corresponding to Configuration 3 of Section III; Ra = 32.6 cm, Rc = 18.5 cm, D1 = 80 cm; V = 20 MV, I = 700 kA, current loss to side anode wall = 80 kA (11%), $\bar{\theta}$ = 17° ± 4°.

the subsequent uniformity of the radiation pattern near the target. The extended planar-anode diode is a limiting case of the indented one where R1 → Ra - Rc and D2 → 0.

In the next sections, we discuss in greater detail the control of the diode impedance, pinch angle, and radiation profiles for several cathode radii at optimized indentations.

As the cathode radius is reduced, a greater fraction of the available radiation is concentrated within a given radius. Simultaneously, however, the energy deposition per unit volume in the target is also increased. This increase results in a higher probability of initiating an anode plasma, which can cause the beam to pinch strongly resulting in degraded radiation uniformity. Additionally, these increases enhance the mechanical stress on the target, which can lead to its destruction and the spread of debris and radioactivity to the upstream regions of the accelerator. Calculations of the expected average energy deposition and preliminary measurements on the HELIA [5] accelerator show, however, that by using thin low-Z foils in front of the target to reduce the temperature rise of the front surface, an anode plasma should not form for the configurations being constructed, if deposition enhancements due to hot spots or filamentation are not large. Calculations also show that by laminating the Ta converter and using graphite as an electron absorber in the target, the tensile stresses in the target can be kept below the spallation threshold. Accordingly, the target should remain intact during a shot, and this issue will not be discussed further here.

*This work was supported by the U. S. Department of Energy under contract DE-AC04-76DP00789.

Report Documentation Page

Form Approved
OMB No. 0704-0188

Public reporting burden for the collection of information is estimated to average 1 hour per response, including the time for reviewing instructions, searching existing data sources, gathering and maintaining the data needed, and completing and reviewing the collection of information. Send comments regarding this burden estimate or any other aspect of this collection of information, including suggestions for reducing this burden, to Washington Headquarters Services, Directorate for Information Operations and Reports, 1215 Jefferson Davis Highway, Suite 1204, Arlington VA 22202-4302. Respondents should be aware that notwithstanding any other provision of law, no person shall be subject to a penalty for failing to comply with a collection of information if it does not display a currently valid OMB control number.

1. REPORT DATE	2. REPORT TYPE	3. DATES COVERED
JUN 1987	**N/A**	**-**

4. TITLE AND SUBTITLE	5a. CONTRACT NUMBER
Indented-Anode Diode For Hermes III	5b. GRANT NUMBER
	5c. PROGRAM ELEMENT NUMBER
6. AUTHOR(S)	5d. PROJECT NUMBER
	5e. TASK NUMBER
	5f. WORK UNIT NUMBER
7. PERFORMING ORGANIZATION NAME(S) AND ADDRESS(ES) **Sandia National Laboratories Albuquerque, New Mexico 87185**	8. PERFORMING ORGANIZATION REPORT NUMBER
9. SPONSORING/MONITORING AGENCY NAME(S) AND ADDRESS(ES)	10. SPONSOR/MONITOR'S ACRONYM(S)
	11. SPONSOR/MONITOR'S REPORT NUMBER(S)

12. DISTRIBUTION/AVAILABILITY STATEMENT
Approved for public release, distribution unlimited

13. SUPPLEMENTARY NOTES
See also ADM002371. 2013 IEEE Pulsed Power Conference, Digest of Technical Papers 1976-2013, and Abstracts of the 2013 IEEE International Conference on Plasma Science. Held in San Francisco, CA on 16-21 June 2013. U.S. Government or Federal Purpose Rights License

14. ABSTRACT
Design of three diode configurations that meet the radiation goals of HERMES III and calculation of associated radiation outputs are discussed. These goals are (1) to produce a 20-ns FWHM radiation pulse having a peak dose rate of 5 x 1012 rad(Si)/s with a variation of less than a factor of two over a 500 em' irradiation area, (2) to keep the variation less than a factor of four over the irradiation volume defined by extending the area downstream by 15 em, and (3) to maintain a minimum dose rate over this volume in excess of 2.5 x 1012 rad(Si)/s.

15. SUBJECT TERMS

16. SECURITY CLASSIFICATION OF:			17. LIMITATION OF ABSTRACT	18. NUMBER OF PAGES	19a. NAME OF RESPONSIBLE PERSON
a. REPORT	b. ABSTRACT	c. THIS PAGE			
unclassified	**unclassified**	**unclassified**	**SAR**	**4**	

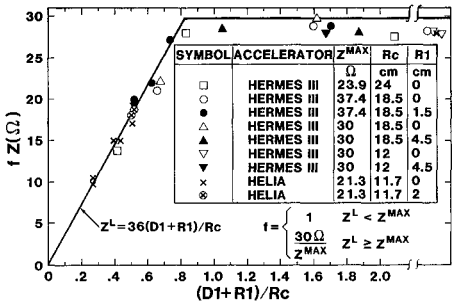

Fig. 3. Comparison of impedance obtained from MAGIC simulation with model described in Section I. Z^{max} corresponds to impedance associated with the minimum current solution [7] of the corresponding MITL/diode simulated.

I. Impedance

Our steady-state MAGIC code [6] simulations and modeling indicate that the planar or indented-anode diode operates in either a load- or a line-dominated regime depending on the AK gap [4] (Fig. 3). In the load-dominated regime, which corresponds to small AK gaps, the impedance is given by

$$Z_{load}^{planar}\ (\Omega) = (36 \pm 4)\ \frac{Dl}{Rc} \qquad (1)$$

for planar-anode diodes. As D2 increases from zero to values exceeding Dl and Rl, which converts the planar anode to an indented anode, our modeling suggests that in the load-dominated regime the diode impedance is still given by Eq. 1, but with Dl replaced by the effective AK gap "Dl + Rl." In this load-dominated regime, the impedance is independent of voltage and surface area of the downstream face of the cathode.

As the effective AK gap is increased, the impedance approaches and equals that associated with the self-limited minimum-current solution of the MITL itself, Zline [7]. In this line-dominated regime, the impedance is independent of the AK gap variables Dl, D2, and Rl. No further increase in impedance with increasing Dl + Rl is possible once Zline is reached.

This dual regime model agrees well with measurements made on HELIA at 3.2 MV [4].

Thus, to run the diode so that it is matched in impedance to the upstream MITL, the effective AK gap need only be larger than a given minimum value. As we show in the next section, the configurations that optimize the radiation pattern have effective gaps well in excess of the minimum value, and are thus automatically matched to the impedance of the MITL.

II. Pinch Angle

In planar-anode diodes having small AK gaps, the electron beam forms a weak pinch owing to the decrease in the radial electric field to zero and the continued presence of the self-magnetic pinching force as the beam approaches the target [8,9]. In a "standard" planar-anode diode that is matched to the 30 Ω MITL, the mean pinch angle is about 41°. CYLTRAN [10] code simulations show that to meet the radiation uniformity goals of HERMES III we need to keep the pinch angle at the target below about 15° [9]. By "indenting" the anode as shown in Fig. 1, or by "extending" the AK gap as shown in Fig. 2, small pinch angles can be achieved, while simultaneously matching the diode to the MITL.

The reduction in pinch angle by indenting or extending the anode is easily understood. Consider first the indented anode of Fig. 1. In the AK gap, the electrons are accelerated from the cathode tip towards the corner of the anode. Because of the self-pinching magnetic force, the electrons can be made to miss the corner and to be injected into the drift space defined by D2 with the proper choice of geometry. If the drift length, D2, is short compared to the axial AK gap, Dl, the beam will continue to pinch because of the shorting-out of the radial electric force at the target. At the other extreme, if D2 is made very large, the beam near the input to the indentation feels essentially the full radial electric field. In this region, the radial electric force is greater than the radial magnetic pinching force by a factor of $1/\beta^2$. β is the speed of the accelerated electrons normalized by the speed of light. As the beam approaches the target, where the radial electric field is necessarily zero, there is still a tendency for the beam to pinch. However, the conditioning of the beam, by adding an outwardly directed component of velocity during the propagation in the drift space, reduces the pinch angle. If D2 is very large, the beam is lost to the side anode wall before it can impact the target. By appropriate choice of D2, however, the effect of the competing radial forces on the beam can be made to partially cancel. This cancellation results in the beam having a more normal angle of incidence at the target. The case of the planar anode that is extended (Fig. 2) is similar except for the injection of the beam into the drift space. In this case, however, control of the diode impedance, by adjustment of Dl + Rl, independent of a given pinch angle, defined by adjustment of D2, is lost.

In both cases, as the beam nears the target, the beam pinches in an axial distance on the order of the gyro radius of the beam in its own magnetic field. The ultimate choice is a tradeoff between achieving the optimum angular and spatial distribution at the target versus minimizing the current loss to the side anode wall. For an indented-anode diode or extended planar-anode diode both matched to the 30 Ω MITL of HERMES III and for beams having similar radial extent at the target of about 22 cm, our simulations show the pinch angle can be reduced to about 22° before current losses to the side anode wall begin (Fig. 4). Further reduction in angle is possible but only at the expense of increased loss. For a given operating voltage, the adjustment between pinch angle and loss to the side anode wall is done by varying D2 for the indented

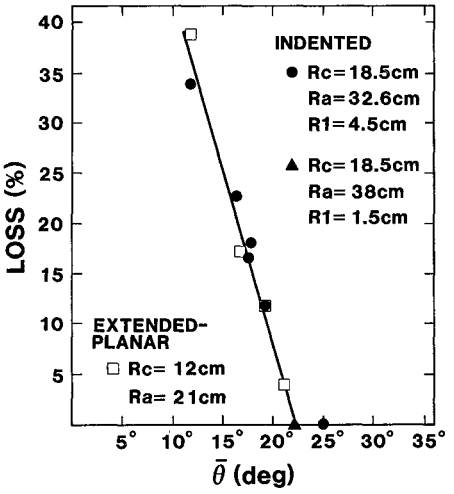

Fig. 4. Percentage of total current lost to side anode wall versus average pinch angle at the target for both an indented and extended planar-anode diode.

anode, or in the case of the extended planar, by varying D1.

For diodes with impedances lower than 30 Ω or beam radii smaller than about 22 cm at the target, the pinch angle for a given loss is higher, because the magnetic force that produces the pinching is larger. Specifically, in the drift region just upstream of the target, where the beam is not scraping the side anode wall, an analysis of the radial force balance at the outside radius of the beam shows that the tangent of the pinch angle at the target is inversely proportional to both the diode impedance and beam radius when the variation in β is neglected. Importantly, if the indented-anode diode is run at a lower impedance by reducing D1 + R1 to increase the magnetic insulation in the MITL, for example, the pinch angle will be larger for a given loss to the side anode wall.

A related point is that at lower voltage β is lower, and the ratio of the radial electric force to magnetic force on the beam electrons is larger. At low voltage, then, the beam is forced into the side anode wall more easily than at high voltage. Consequently, electrons of lower energy associated with the leading and trailing edges of the voltage pulse are prevented from reaching the target. Thus, the indentation provides a degree of radiation pulse sharpening.

III. Radiation Profiles

The primary goals of HERMES III are (1) to produce a 20-ns FWHM radiation pulse having a peak dose rate, $\dot{D}$, of 5 x 10^{12} rad(Si)/s with a variation of less than a factor of two over a 500 cm² irradiation area, (2) to keep the variation less than a factor of four over the irradiation volume defined by extending the area downstream by 15 cm, and (3) to maintain a minimum dose rate over this volume in excess of 2.5 x 10^{12} rad(Si)/s. These peak dose rate and uniformity goals can be achieved by using matched indented- or extended planar-anode diodes operating at voltages in excess of 20 MV where the geometry is optimized such that the pinch angle is kept between about 20° to 15°, and where the losses to the side anode wall are less than 25%. This optimization results in tolerable losses that still permit the peak dose rate and uniformity goals to be simultaneously achieved. The peak operating voltage of the accelerator of 22.5 MV [2] is 10% higher than the roughly 20 MV needed to meet the primary goals and provides an added safety factor enabling HERMES III to meet its design goals. By adjusting the radial extent of the beam at the converter, this safety factor can be used to either increase intensity over the 500 cm² area or increase the uniformity over a larger area.

Within the framework of these primary goals, we have designed three configurations that enable the goals to be met with either enhanced intensity capability (small radius) or enhanced uniformity capability (large radius) (Tables I and II). All designs require a slight taper in the upstream MITL (Ra = 38.1 cm, Rc = 21.6 cm) to reach the required diode radii.

Table I. Optimized Diode Configurations

Configuration	Type	Rc cm	Ra cm	R1 cm	D1 cm	D2 cm	Figs.
1	Indented	12	21	5	15	30	5
2	Indented	18.5	32.6	4.5	30	40	1,5
3	Extended	18.5	32.6	--	80	--	2,5

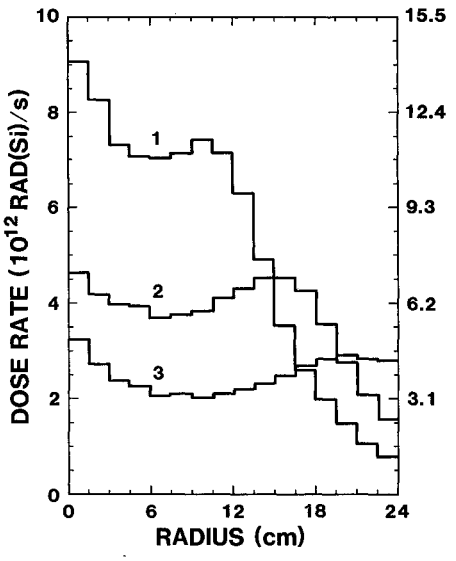

Fig. 5 Comparison of radial radiation profiles at peak voltage in a plane 10 cm downstream of upstream target face for Configurations 1, 2, and 3 of Section III. Scale on left corresponds to 20 MV peak voltage, and scale on right corresponds to 22.5 MV peak voltage.

A comparison of the expected radiation output corresponding to the three configurations is shown in Fig. 5 and Table II. The output was calculated using MAGIC to simulate the spatial and angular distribution of the electrons in the diode at 20 MV and CYLTRAN to track the subsequent electromagnetic shower in the target, side anode walls, and vacuum chamber. In MAGIC, a voltage pulse of 1 ns rise time was used. Once MAGIC reached a steady-state flow, its output was used as input to CYLTRAN. The geometry used in CYLTRAN corresponded to that being constructed. It consists of an optimized bremsstrahlung target made of .5 ER (CSDA electron range) of Ta followed by .75 ER of graphite [11], side anode walls made of 7 cm thick graphite, and a 1 cm thick Al vacuum chamber.

Configuration 1 has the smallest radial extent of the beam. The electron distribution peaks between 10 cm and 15 cm at the Ta converter, and the peak surface deposition is about 60 J/gm when averaged over 1 to 2 cm radial bins. This configuration just meets the uniformity requirement (Table II) but maximizes the available intensity over 500 cm². If peak voltages are not initially reached, operation at only 18 MV will still enable the goals to be met with this configuration. At the other extreme, configuration 3 has the largest radial extent of the beam. The electron distribution peaks between 17 cm and 32.6 cm at the Ta converter, and the peak surface deposition is about 20 J/gm when averaged over 1 to 2 cm bins. This configuration just meets the intensity requirement (Table II) but maximizes the uniformity over the largest area. Even for Configuration 1, the expected energy depositions are low enough that ion plasma formation and target destruction due to spallation should not be a problem. However, if hot spots or filamentation increase local depositions, Configuration 3 can provide an average deposition reduction of a factor of 3 relative to Configuration 1 and still enable the primary radiation goals to be met at 22.5 MV.

Configuration 2 falls midway between the two extremes. The extended planar-anode of Configuration 3 with Rc = 18.5 cm is a natural extension of indented anode of Configuration 2 with Rc = 18.5 cm. It is also capable of providing the secondary large-area exposure

Table II. Comparison of radiation output for 30 Ω optimized diode configurations of Table I with design goals for 20 MeV and 22.5 MeV incident electrons.

Configuration	V	Area	Over Area			Over Area x 15 cm Volume	
			$\bar{\dot{D}}$	$\dot{D}^{max}$	$\dot{D}^{max}/\dot{D}^{min}$	$\dot{D}^{min}$	$\dot{D}^{max}/\dot{D}^{min}$
	MV	cm²	10^{12} rad(Si)/s	10^{12} rad(Si)/s		10^{12} rad(Si)/s	
Goal		500	--	5.0	2.0	2.5	4.0
1	20	500	7.0	9.0	1.5	3.0	3.0
	22.5	500	11.0	14.0	1.5	4.7	3.0
2	20	500	4.0	4.6	1.3	3.3	1.5
	22.5	500	6.2	7.2	1.3	5.1	1.5
3	20	1800	2.5	3.2	1.6	1.6	2.1
	22.5	1800	3.9	5.0	1.6	2.5	2.1
	20	10,000	.15	.18	1.4		
	22.5	10,000	.23	.29	1.4		
	20	100,000	.027	.036	2.0		
	22.5	100,000	.042	.056	2.0		

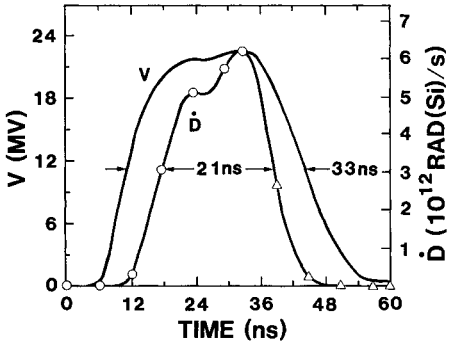

Fig. 6. (V) Expected voltage pulse at diode/MITL interface for HERMES III operating at upper end of safe-operating range. (Ḋ) Associated radiation pulse from Configuration 2 averaged over 500 cm² just downstream of target.

goals [1] and will provide the load, with the Ta converter replaced by graphite in the target, as HERMES III is being commissioned. Indented-anode Configuration 1 with Rc = 12 cm requires an additional taper in the MITL relative to Configuration 2.

Figure 6 shows the expected voltage pulse at the diode/MITL interface for HERMES III running at the upper end of its safe-operating range. The pulse has a peak value of 22.5 MV with a FWHM of 33 ns. Shown also in the figure is the associated radiation pulse averaged over 500 cm² just downstream of the target as calculated using the MAGIC and CYLTRAN codes for Configuration 2. The average pulse has a peak value of 6.2 x 10^{12} rad(Si)/s with a FWHM of 21 ns. The integrated dose under the pulse is 122 krad(Si). In the calculations, account is taken of the change in the voltage, electron flow pattern, losses, and interactions in the side anode wall and target as a function of time. Further reduction in the width of the radiation pulse may be achieved by using either self-breaking crowbar switches in the pulse-forming lines or plasma-opening switches just upstream of the diode [1,2].

Summary

In summary, the three diode configurations provide loads that can be partially decoupled from the optimization of the radiation source. The configurations provide flexibility in meeting a given radiation need within the design goals. They also provide safety in achieving those goals if either low voltages are encountered or if an anode plasma is formed at our highest energy deposition.

Acknowledgements

We would like to thank K. R. Prestwich and J. J. Ramirez for useful discussions, W. P. Ballard for reviewing the paper, and M. Song for typing it.

References

[1] J. J. Ramirez, et al, "The HERMES III Program," in these proceedings.
[2] R. C. Pate, et al, "Self-Magnetically Insulated Transmission Line (MITL) System Design for the 20-Stage HERMES III Accelerator," in these proceedings.
[3] T. W. L. Sanford, et al, Appl. Phys. Lett. 50, 809 (March 30, 1987).
[4] T. W. L. Sanford, et al, Int'l. Conf. on Plasma Sci., Arlington, VA, (June 1-3, 1987), IEEE Catalog No. 878CH2451-3, 25.
[5] J. J. Ramirez, et al, in Proc. of the 5th IEEE Pulse Power Conf., Arlington, VA, IEEE Catalog No. 852121-2, 143 (1985).
[6] B. Goplen, et al, Mission Research Corporation, Report No. MRC /WDC-R-068, Alexandria, VA (September 1983).
[7] J. M. Creedon, J. Appl. Phys. 46, 2946 (July 1975).
[8] T. W. L. Sanford, et al, Int'l. Conf. on Plasma Sci., Saskatoon, Canada, (May 19-21, 1986), IEEE Catalog No. 86CH2317-6, 45.
[9] T. W. L. Sanford, J. A. Halbleib, J. W. Poukey, and T. P. Wright, Sandia National Laboratories Report, SAND85-2383 (January 1987).
[10] J. A. Halbleib and T. A. Mehlhorn, Nucl. Sci. Eng. 92, 338 (1986).
[11] T. W. L. Sanford and J. A. Halbleib, IEEE Trans. Nucl. Sci., Vol. NS-31, No. 6, 1095 (Dec. 1984).